Evolutionary Dynamics of *Vibrio cholerae* O1 following a Single-Source Introduction to Haiti

Lee S. Katz,[a] Aaron Petkau,[b] John Beaulaurier,[c] Shaun Tyler,[b] Elena S. Antonova,[d] Maryann A. Turnsek,[a] Yan Guo,[e] Susana Wang,[e] Ellen E. Paxinos,[e] Fabini Orata,[f] Lori M. Gladney,[a] Steven Stroika,[a] Jason P. Folster,[a] Lori Rowe,[a] Molly M. Freeman,[a] Natalie Knox,[b] Mike Frace,[a] Jacques Boncy,[g] Morag Graham,[b] Brian K. Hammer,[d] Yan Boucher,[f] Ali Bashir,[c] William P. Hanage,[h] Gary Van Domselaar,[b] Cheryl L. Tarr[a]

Centers for Disease Control and Prevention, Atlanta, Georgia, USA[a]; National Microbiology Laboratory, Public Health Agency of Canada, Winnipeg, Manitoba, Canada[b]; Department of Genetics and Genomics Sciences, Mount Sinai School of Medicine, New York, New York, USA[c]; School of Biology, Georgia Institute of Technology, Atlanta, Georgia, USA[d]; Pacific Biosciences, Menlo Park, California, USA[e]; Department of Biological Sciences, University of Alberta, Edmonton, Alberta, Canada[f]; National Public Health Laboratory, Port-au-Prince, Haiti[g]; Center for Communicable Disease Dynamics, Department of Epidemiology, Harvard University, Boston, Massachusetts, USA[h]

ABSTRACT Prior to the epidemic that emerged in Haiti in October of 2010, cholera had not been documented in this country. After its introduction, a strain of *Vibrio cholerae* O1 spread rapidly throughout Haiti, where it caused over 600,000 cases of disease and >7,500 deaths in the first two years of the epidemic. We applied whole-genome sequencing to a temporal series of *V. cholerae* isolates from Haiti to gain insight into the mode and tempo of evolution in this isolated population of *V. cholerae* O1. Phylogenetic and Bayesian analyses supported the hypothesis that all isolates in the sample set diverged from a common ancestor within a time frame that is consistent with epidemiological observations. A pangenome analysis showed nearly homogeneous genomic content, with no evidence of gene acquisition among Haiti isolates. Nine nearly closed genomes assembled from continuous-long-read data showed evidence of genome rearrangements and supported the observation of no gene acquisition among isolates. Thus, intrinsic mutational processes can account for virtually all of the observed genetic polymorphism, with no demonstrable contribution from horizontal gene transfer (HGT). Consistent with this, the 12 Haiti isolates tested by laboratory HGT assays were severely impaired for transformation, although unlike previously characterized noncompetent *V. cholerae* isolates, each expressed *hapR* and possessed a functional quorum-sensing system. Continued monitoring of *V. cholerae* in Haiti will illuminate the processes influencing the origin and fate of genome variants, which will facilitate interpretation of genetic variation in future epidemics.

IMPORTANCE *Vibrio cholerae* is the cause of substantial morbidity and mortality worldwide, with over three million cases of disease each year. An understanding of the mode and rate of evolutionary change is critical for proper interpretation of genome sequence data and attribution of outbreak sources. The Haiti epidemic provides an unprecedented opportunity to study an isolated, single-source outbreak of *Vibrio cholerae* O1 over an established time frame. By using multiple approaches to assay genetic variation, we found no evidence that the Haiti strain has acquired any genes by horizontal gene transfer, an observation that led us to discover that it is also poorly transformable. We have found no evidence that environmental strains have played a role in the evolution of the outbreak strain.

Address correspondence to Cheryl L. Tarr, ctarr@cdc.gov.

*V*ibrio cholerae is a pathogen of considerable public health concern because of its potential to cause large epidemics and pandemics and its high case fatality rate when the disease is left untreated. The disease cholera is caused by *V. cholerae* strains of serogroups O1 and O139 that can produce a potent enterotoxin, cholera toxin, which is encoded by the *ctxAB* genes on the bacteriophage CTXφ (1). Seven pandemics of cholera have been recorded since 1817, when the disease first emerged from the Bay of Bengal and spread around the globe (2). The current seventh pandemic of *V. cholerae* originated in Southeast Asia and has spread across the globe in several waves of transmission (3). In October of 2010, cholera made its appearance in Haiti. Prior to 2010, there were no documented cases of cholera in that country, despite the devastating outbreaks occurring in the Caribbean in the 19th century (4). Its introduction to the island of Hispaniola following the earthquake that occurred there in January of 2010 has resulted in the largest epidemic of cholera in recent times: 604,634 cases and 7,436 deaths were documented in the first two years of the epidemic (5).

Initial epidemiological and genetic studies focused on the origin of the Haiti epidemic and quickly attributed the outbreak to human introduction of a *V. cholerae* O1 strain from outside the

region, most likely South Asia (6, 7). Epidemiological investigations pointed to Nepalese troops serving as United Nations (UN) peacekeepers as the source of cholera, based on reports of unsanitary conditions at the UN camp, the spatial-temporal pattern of disease clusters, and the coincidence of the outbreak with the arrival of the UN troops from Nepal (8). Phylogenetic analysis of time-relevant isolates from Haiti and Nepal provided additional support for the hypothesis that the epidemic strain was imported from Nepal (9).

The single-source introduction and geographic isolation of the Haiti epidemic, along with the extended duration of the outbreak, provide an unprecedented natural experiment for characterizing in detail the intrinsic tempo and mode of genome evolution in this deadly pathogen. We performed whole-genome sequencing on a set of well-characterized isolates collected near or after the 1-year anniversary date of the Haitian outbreak, and compared them with isolates collected early in the epidemic to gain insight into the dynamics of genome evolution in *V. cholerae* O1. The sample set includes isolates collected at different time points and in different localities (9, 10) as well as phenotypically and genotypically distinct isolates discovered during routine laboratory surveillance by the Centers for Disease Control and Prevention. The variants that have arisen in the course of the outbreak include various pulsed-field gel electrophoresis (PFGE) pattern combinations, serotype Inaba (11), an altered antibiotic susceptibility pattern (ASP), and a nonagglutinating (NAG) *V. cholerae* strain. We first conducted phylogenetic analysis to determine whether the diverse set of isolates were all part of the same outbreak and then used the genome sequences to compare gene content and structural arrangement of chromosomes.

RESULTS

We sequenced 23 genomes on the Illumina platform (see Table S1 in the supplemental material). The sample set represents geographically dispersed isolates collected over an array of time points and representing multiple PFGE pattern combinations (see Fig. S1 to S3 in the supplemental material). Eighty-seven genomes were downloaded from the Sequence Read Archive (SRA) (see Table S2 in the supplemental material); two were found to have >20% non-*Vibrio* genetic material and were excluded from the study: hc-17a1 and hc-77a1. Comparing the 108 genomes yielded 566 core genome single-nucleotide polymorphisms (SNPs). Of the 23 isolates, we sequenced 9 on the PacBio platform and resequenced the reference strain 2010EL-1786.

A phylogenetic tree constructed from the 566 core SNPs grouped all Haiti isolates and three Nepal isolates (14, 25, 26) in a single monophyletic group within the context of a global collection of 108 *Vibrio cholerae* O1 strains (see Fig. S4 in the supplemental material). Next, we uncovered 45 high-quality SNPs (hqSNPs) in the Haiti-Nepal group. The minimum spanning tree (MST) constructed from the hqSNPs was concordant with the clustering of isolates by maximum likelihood analysis (Fig. 1; also, see Fig. S4 in the supplemental material). The MST illustrated the radiation of numerous lineages from a single sequence type that predominated in the early part of the epidemic.

We then examined the 45 hqSNPs for potential effects on function (see Table S3 in the supplemental material). Most notable was a GAA-to-TAA substitution in the *wbeT* gene of 2012EL-1410, a representative of five serotype Inaba isolates from our Haiti collection. The substitution introduces a premature stop codon into

the gene, which predicts a truncated protein, a result that is consistent with other studies showing that serotype conversion results from mutations in the *wbeT* gene (12). Comparison of three different molecular clock models showed that overall the changes at nucleotide sites were consistent with the epidemic behavior, as the highest likelihood was obtained under the exponential growth model. Using a strict molecular clock, analysis of 10^8 states from eight independent runs yielded a median estimate of the date of the most recent common ancestor to be 28 September 2010 (95% credible interval, 23 July 2010 to 17 October 2010).

Variation in gene content and structural arrangement. Few differences in gene content were observed (Fig. 2). The BLAST atlas showed no evidence of gene acquisition, but a few deletions were apparent, and the assembly of long reads showed similar results. In addition, three large inversions in or around the SXT region were evident in the long-read assemblies (Fig. 3). Amplification across the 3′ end of the inversion boundaries in isolates with rearrangements and in the reference strain 2010EL-1786 confirmed the structural variation observed in the assemblies.

Quorum sensing and transformation. To determine whether the Haiti clone was capable of natural transformation, one mechanism of horizontal gene transfer (HGT), standard laboratory DNA uptake assays (18) were performed on twelve isolates. Virtually no kanamycin-resistant (Kanʳ), Lac⁻ transformants were detected (Table 1) for Haiti isolates in assays using DNA from reference *V. cholerae* strain C6706 with a *kan* gene disrupting the *lacZ* gene (14). C6706, which is capable of quorum sensing (QS), transformed at an efficiency 10^3 to 10^4 times greater than that of each of the Haiti isolates and a QS-deficient C6706 Δ*hapR* strain. Similar results were observed when we attempted to transform each Haiti isolate with its own *kan* genomic DNA (Table 2), or with C6706 genomic DNA with an ampicillin resistance gene disrupting the *lacZ* gene (data not shown). Thus, it appears that the Haiti clone not only failed to acquire any genes by HGT but also was poorly transformable by standard laboratory DNA uptake assays. We examined the sequences of 47 genes that are involved in the QS and other signaling systems known to control transformation (14); each gene was present, and there were no loss-of-function or nonsense mutations in these genes or their promoters (data not shown). Also, each Haiti isolate was experimentally shown to be QS proficient, as expression of a QS-dependent reporter gene introduced into each of the 12 Haiti strains was similar to that of the positive control (PC) C6706 strain, while the negative control (NC) C6706 Δ*hapR* strain was ≥1,000-fold impaired, which corresponds to the detection limit (data not shown).

DISCUSSION

We used genomic approaches to characterize evolutionary changes in the *V. cholerae* O1 population following the introduction to Haiti. Our results were consistent with previous findings that show that the Haiti cholera outbreak is clonal and that Nepalese isolates are the closest relatives to the Haiti strain identified to date (9), even when placed in a phylogeny with a larger collection of isolates representing recent cholera epidemics. A previous study based on WGS (9) showed that Nepalese isolates were almost indistinguishable from Haiti isolates; however, that phylogeny did not include isolates recovered from recent cholera outbreaks. The phylogeny presented here provides evidence that the observed variants that were detected by our surveillance are part of the same outbreak and not representatives of secondary introduc-
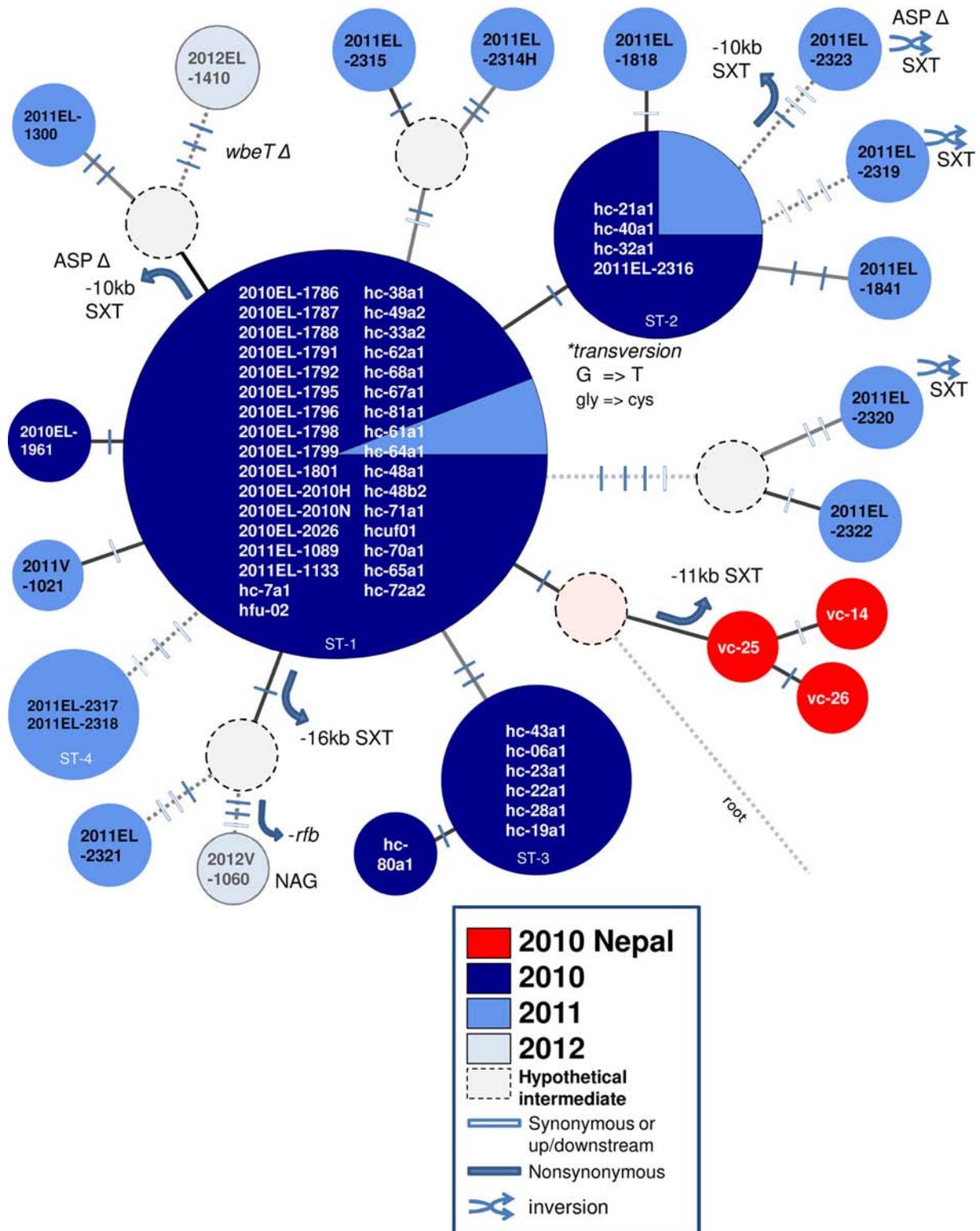
FIG 1 Minimum spanning tree (MST) constructed from 45 hqSNPs. Intermediate hypothetical ancestors were inferred for some lineages and manually placed in the network. Nucleotide substitutions are indicated by dashes along the branches, and deletion events are indicated by arrows. ASP, antimicrobial susceptibility pattern. The ~10 kb deletion in the SXT is inferred twice in the model, and occurs between two transposase genes, VCH1786_I0078 and VCH1786_I0087. *, nonsynonymous transversion.
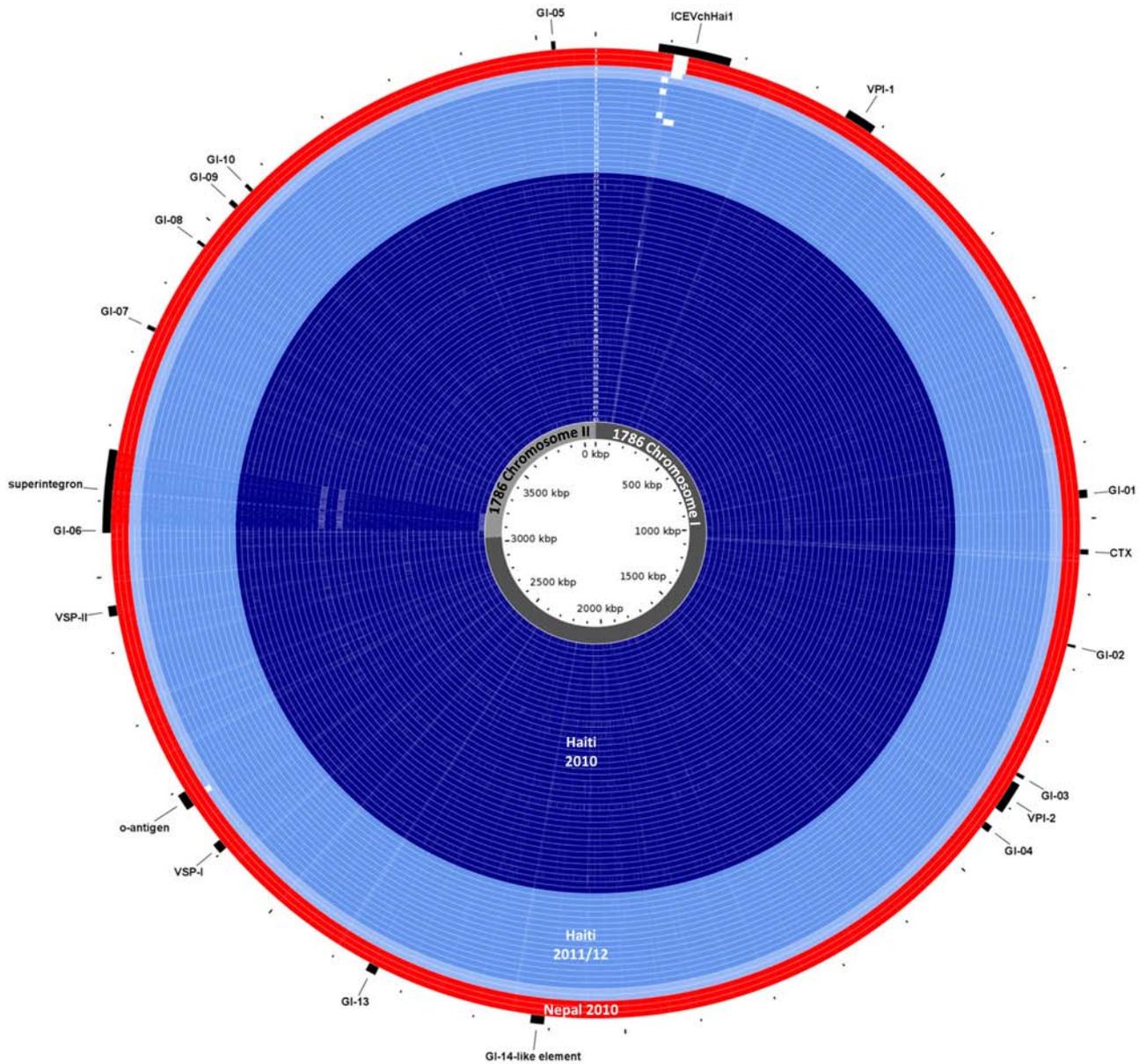
Isolates

1 - vc-25	11 - 2011EL-1300	21 - 2011V-1021	31 - hc-32a1	41 - 2010EL-1801	51 - hc-62a1	61 - hcuf01
2 - vc-14	12 - 2011EL-2321	22 - 2010EL-1961	32 - hc-21a1	42 - 2010EL-2010H	52 - hc-64a1	62 - hfu-02
3 - vc-26	13 - 2011EL-2322	23 - hc-80a1	33 - 2010EL-1787	43 - 2010EL-2010N	53 - hc-65a1	63 - 2010EL-1786
4 - 2012V-1060	14 - 2011el-2320	24 - hc-43a1	34 - 2010EL-1788	44 - 2010EL-2026	54 - hc-67a1	
5 - 2012EL-1410	15 - 2011EL-2318	25 - hc-28a1	35 - 2010EL-1791	45 - hc-33a2	55 - hc-68a1	
6 - 2011EL-2316	16 - 2011EL-2317	26 - hc-23a1	36 - 2010EL-1792	46 - hc-38a1	56 - hc-70a1	
7 - 2011EL-2323	17 - 2011EL-2315	27 - hc-22a1	37 - 2010EL-1795	47 - hc-48a1	57 - hc-71a1	
8 - 2011EL-1841	18 - 2011EL-2314H	28 - hc-19a1	38 - 2010EL-1796	48 - hc-48b2	58 - hc-72a2	
9 - 2011EL-1818	19 - 2011EL-1089	29 - hc-06a1	39 - 2010EL-1798	49 - hc-49a2	59 - hc-7a1	
10 - 2011EL-2319	20 - 2011EL-1133	30 - hc-40a1	40 - 2010EL-1799	50 - hc-61a1	60 - hc-81a1	

FIG 2 BLAST atlas. Genes from each *de novo* assembly were compared against both chromosomes of the completed genome 2010EL-1786. Absence of color (white) indicates that a strain is missing genetic material that is present in the reference. Regions of interest are denoted by black rectangles on the circumference. Three genomes have a shorter Illumina read length (36 bp), which might have resulted in fewer gene predictions, which manifests as an artifact on the atlas in the superintegron region. The isolate names are listed from the outermost to the innermost tracks.
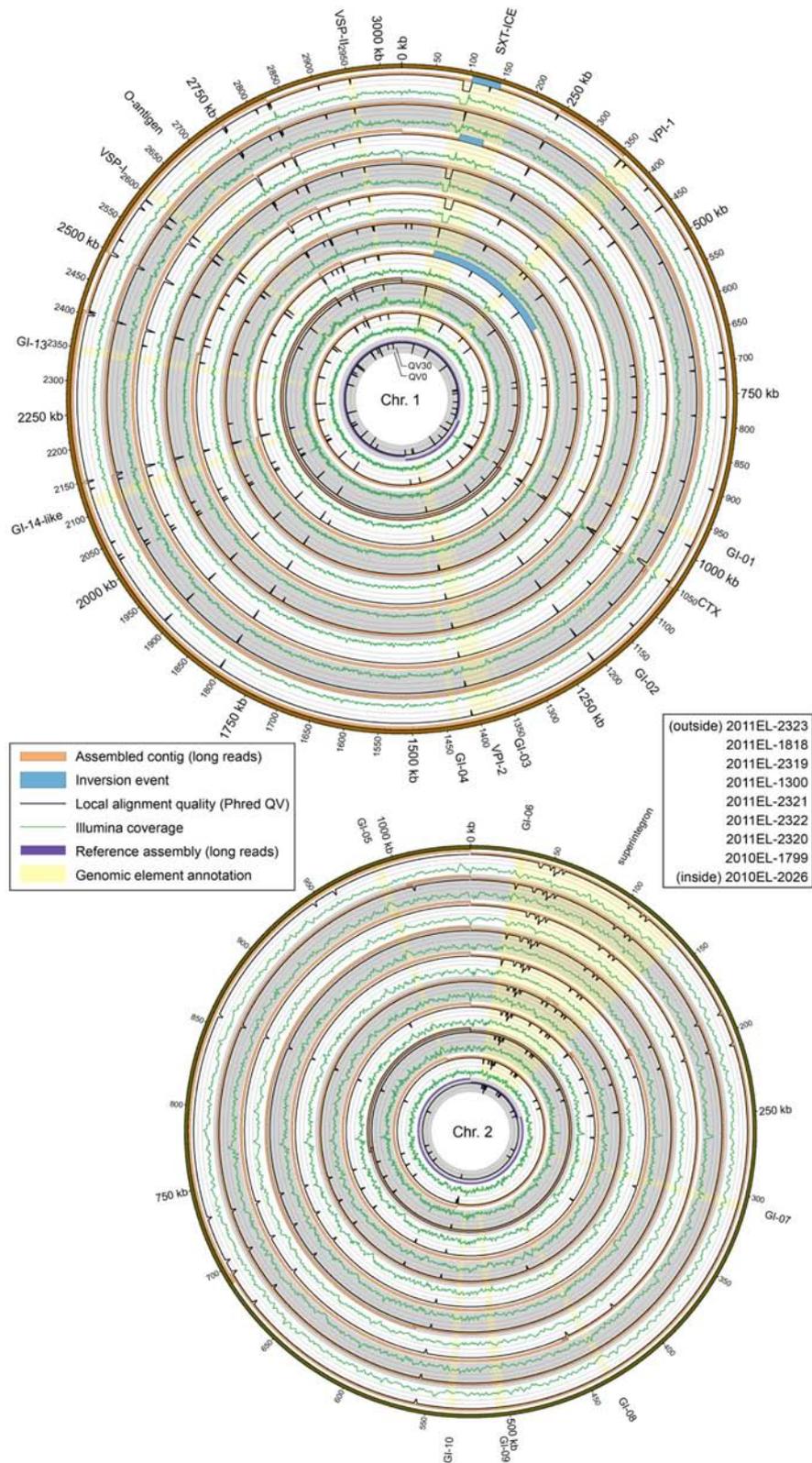
FIG 3 Circos plot showing structural genome rearrangements. Each alternating white/gray band represents one of the nine strains sequenced on the PacBio RS platform, with an inner tenth track representing the published reference strain (7). Each band contains three tracks. The outermost, orange tiles represent contigs from *de novo* assemblies aligned back to the 2010EL-1786 reference. Inversions within contigs are highlighted in blue. Black line plots show local alignment quality over 1kb windows, in terms of Phred QV, for long read assembled contigs compared to the 2010EL-1786. Note the smallest dips in QV correspond to single SNPs. Green line plots show local coverage of Illumina short reads mapped to the reference over 500bp windows. The innermost band contains a purple track showing contigs from a separate long read *de novo* assembly of 2010EL-1786. The black QV track highlights differences between the long read and short assembly, indicating potential areas of misassembly in the original reference.

TABLE 1 Haiti isolates are defective for transformation with C6706 gDNA with *kan* at *lacZ*

gDNA	Recipient strain	TF[a]	Range[b]	Fold reduction[c]
C6706*lacZ*(*kan*)	C6706	<1.3E-5	1.9E-5–7.8E-6	1
C6706*lacZ*(*kan*)	2010EL-1786	<3.8E-9	–	>3,428
C6706*lacZ*(*kan*)	2010EL-1799	<2.5E-9	–	>5,200
C6706*lacZ*(*kan*)	2010EL-2026	<1.9E-9	–	>6,948
C6706*lacZ*(*kan*)	2011EL-1818	<1.6E-9	–	>8,196
C6706*lacZ*(*kan*)	2011EL-1841	<1.5E-9	–	>8,392
C6706*lacZ*(*kan*)	2011EL-2319	<5.4E-9	–	>2,399
C6706*lacZ*(*kan*)	2011EL-2320	<1.3E-9	–	>9,588
C6706*lacZ*(*kan*)	2011EL-2321	<1.4E-9	–	>9,508
C6706*lacZ*(*kan*)	2011EL-2322	<3.6E-9	<DL–8.6E-9	>3,621
C6706*lacZ*(*kan*)	2011EL-2323	<1.8E-9	–	>7,223
C6706*lacZ*(*kan*)	2012EL-1410	<7.3E-10	–	>17,648
C6706*lacZ*(*kan*)	2011EL-1300	<9.5E-10	–	>13,635
C6706*lacZ*(*kan*)	C6706 Δ*hapR*	<6.5E-9	–	>2,001

[a] TF, average transformation frequency from triplicate samples.
[b] DL (detection limit) was <1.0E-8 for all experiments. "–" indicates transformants below the DL. 1 CFU rather than 0 was used to calculate TF.
[c] Fold reduction = TF of recipient/TF of C6706.

tions. The synthesis of PFGE and sequence data demonstrated the utility of WGS in establishing the clonality of isolates that exhibit greater PFGE dissimilarity than would normally be attributed to a single-source outbreak. The use of high-resolution sequence data that are amenable to evolutionary analysis will greatly enhance our ability to discern transmission pathways of virulent clones, such as the one implicated in this epidemic.

The nucleotide polymorphism that we detected was consistent with the observed epidemic behavior, as the most supported model of population growth was exponential. The molecular clock calculated with this model estimated a most recent common ancestor date of 28 September 2010 (95% credibility interval [CI], 23 July 2010 to 17 October 2010) (see Fig. S5 in the supplemental material). The credibility interval encompasses the date that the Nepalese soldiers arrived in Haiti (9 October 2010) (8), as well as the first reported hospitalization of a cholera case (17 October 2010) (although an earlier fatal case with an onset date of 12 October may have been the index case) (15). The consistency between the molecular data and the epidemiological information demonstrates the utility of advanced statistical tools in outbreak investigations where epidemiological information may be lacking. Our results suggest that a population genomic approach can be very powerful in delimiting the time frame of an outbreak.

We observed remarkably few differences in the genetic repertoire of the *V. cholerae* O1 population (Fig. 2). All genes from Haiti isolates were found in the genome of the reference strain (2010EL-1786), and the differences in gene content could be attributed to loss of genetic material. The NAG isolate (2012V-1060) had a unique ~10-kb deletion, and closer examination revealed that several key components were missing from the *rfb* region (see Fig. S6 in the supplemental material). The isolate therefore appeared to be a serogroup O1 strain that was unable to synthesize or transport O antigen to the cell surface. Five representative strains were observed to have large deletions in the SXT, an ~100-kb integrative conjugative element that exhibits considerable diversity in gene content (16). One ~10-kb SXT deletion was found in three isolates (Fig. 1; also, see Fig. S7 in the supplemental material) that also shared an altered ASP. The typical ASP for Haiti *V. cholerae* includes intermediate resistance to chloramphenicol and nonsusceptibility to streptomycin, sulfisoxazole, trimethoprim/sulfame-

thoxazole, and nalidixic acid, resistance traits that are encoded by *floR*, *strA*, *strB*, *sul2*, *dfrA1*, and a point mutation in *gyrA* (17). The isolates with the altered ASP displayed nonsusceptibility only to nalidixic acid, and both PCR and genome analysis confirmed the loss of *floR*, *strA*, *strB*, and *sul2* resistance genes in the SXT region of these isolates. The deletion could not be placed parsimoniously on the MST (Fig. 1); however, it falls within variable region III (16) (see Fig. S7) and is flanked by transposase genes, so it is reasonable to suppose that the same deletion occurred independently in two different lineages. The SXT deletion could be made parsimonious by inferring that the nonsynonymous transversion (Fig. 1, asterisk) reverted to its original state, an event that we concluded is less likely to occur. We note that a parsimonious reconstruction indicates loss of SXT genes in the three closest Nepal isolates after divergence from the common ancestor of the Nepal-Haiti cluster (Fig. 1), as the other two most closely related Nepal lineages from Hendriksen et al. (9) (Nepal-2 and Nepal-3) possess an intact SXT (see Fig. S7). The large deletions in the SXT and *rfb* regions (Fig. 3) were confirmed by the continuous-long-read (CLR) assemblies. The nearly complete assemblies from the CLR and the BLAST atlas were both consistent with the notion that the Haiti *V. cholerae* strain has not acquired genes or genomic islands. Thus, we found no evidence that unrelated bacterial strains in the environment have contributed to the diversification of the Haiti outbreak strain.

It is well accepted that HGT is a major force driving evolution in bacteria, including *Vibrio* (18, 19); thus, the lack of HGT observed in our study might be surprising. Limited data suggest that changes can accumulate over a relatively short time frame (20), and a previous study of *V. cholerae* from Haiti (10) reported accumulation of diversity early in the epidemic although gene acquisition was not specifically demonstrated in *V. cholerae* serogroup O1. In *Vibrio cholerae*, natural transformation, an important mechanism of HGT, occurs on chitinous surfaces and requires quorum sensing (QS) (i.e., the HapR QS transcription factor) (13, 14). Thus, we first considered whether transmission dynamics precluded the establishment of epidemic *V. cholerae* in the environment so that they lacked exposure to other *Vibrio* and to chitin, which are critical for HGT by transformation (12). Although it is possible that environmental factors could limit HGT between en-

TABLE 2 Haiti isolates are defective for transformation with self-derived *tn*(*kan*) gDNA[a]

gDNA donor	Test sample			Control			Fold reduction[b]
	Recipient strain	TF	Range	Recipient strain	TF	Range	
2010EL-1786	2010EL-1786	<5.1E-9	–	C6706	5.3E-6	4.7E-6–5.7E-6	>1,046
2010EL-1799	2010EL-1799	<2.1E-9	–	C6706	1.8E-5	1.1E-5–1.9E-5	>8,462
2010EL-2026	2010EL-2026	<1.7E-9	–	C6706	6.0E-6	1.8E-6–1.0E-6	>3,484
2011EL-1818	2011EL-1818	<2.1E-9	<DL-2.5E-9	C6706	1.4E-5	8.8E-6–1.9E-5	>6,842
2011EL-1841	2011EL-1841	<8.1E-9	<DL-1.3E-8	C6706	1.9E-5	1.2E-5–2.5E-5	>2,314
2011EL-2319	2011EL-2319	<2.0E-9	–	C6706	1.4E-5	5.6E-6–1.7E-5	>7,087
2011EL-2320	2011EL-2320	<1.9E-9	–	C6706	1.7E-5	1.1E-5–1.8E-5	>8,826
2011EL-2321	2011EL-2321	<5.4E-9	<DL-9.9E-9	C6706	1.9E-5	9.3E-6–6.2E-5	>3,437
2011EL-2322	2011EL-2322	<5.7E-9	<DL-3.3E-9	C6706	1.0E-5	1.1E-6–2.3E-5	>1,789
2011EL-2323	2011EL-2323	<3.7E-9	<DL-1.9E-9	C6706	1.1E-5	4.7E-6–1.1E-5	>2,966
2012EL-1410	2012EL-1410	<4.2E-9	–	C6706	4.8E-5	3.7E-6–5.6E-6	>1,161
2011EL-1300	2011EL-1300	<1.6E-9	–	C6706	9.4E-6	5.7E-6–1.4E-5	>5,960
2011EL-1300	C6706 Δ*hapR*[c]	<6.4E-9	–	C6706	9.4E-6	5.7E-6–1.4E-5	>1,476

[a] TF, DL, and – are as defined in Table 1.

[b] Fold reduction = TF(test)/TF(control).

[c] The C6706 Δ*hapR* recipient was transformed with gDNA from 2011EL-1300.

vironmental and epidemic *V. cholerae*, they are likely in contact, as coisolation has been observed on several occasions from environmental and clinical samples (10) (Vince Hill [CDC], personal communication). We therefore tested the alternative hypothesis that the Haiti *V. cholerae* strain could be deficient in natural transformation and therefore unable to take up and incorporate foreign DNA. The transformation experiments on chitin showed that unlike naturally competent clinical strain C6706, each Haiti isolate was severely impaired in its ability to take up extracellular DNA derived from C6706 (Table 1) or from itself (Table 2). Further experiments confirmed that the isolates, like C6706, were quorum-sensing proficient and expressed *hapR* (data not shown). Thus, the Haiti strain appears to be limited in its ability to acquire new genetic material through transformation, but this is not due to QS deficiencies, as have been identified in other nontransformable *V. cholerae* isolates (13) (B. K. Hammer and E. E. Bernardy, unpublished results). It remains possible that *V. cholerae* isolates defective for transformation in lab settings may, nonetheless, be naturally competent in nature. However, to our knowledge no such strains have yet been described. Also, a longer time frame may be required for recombination to occur with more distantly related lineages and create mosaics that are successful enough to be observed. We note that the low rates of transformation would presumably not affect HGT via other mechanisms such as phage transduction or conjugation.

In summary, the Haiti cholera epidemic provided a unique opportunity to study the evolutionary dynamics of an isolated population of *V. cholerae* O1. Although PFGE was initially critical for determining that a single strain caused the outbreak, subsequent changes in PFGE patterns precluded our ability to determine that observed variants traced back to a single epidemic founder, an issue that was addressed by using WGS in our comprehensive surveillance strategy. The sample set was virtually homogeneous in gene content, an observation that led to the discovery that the Haiti strain is poorly transformable. Thus, our study indicates that transformation by unrelated environmental strains of *V. cholerae* has played no detectable role in the evolution of the outbreak strain. Further studies will define the genetic mutation(s) that rendered the Haiti strain defective in HGT via natural transformation. Once the mutation(s) is identified, its temporal

origin and global prevalence can be determined to understand more about the stability and success of this particular genotype and the role that transformation plays in its genome evolution and success in establishing itself in a new environment. Atypical O1 El Tor *V. cholerae* strains such as the Haiti strain have already displaced prototypical El Tor strains and emerged as the predominant clone circulating in Asia and Africa (21–24). These strains have acquired multidrug resistance and enhanced virulence traits such as classical or hybrid CTX prophage and SXT-ICE, resulting in higher infection rates and harsher symptoms (25). With the tools such as WGS now being available for epidemiological surveillance and case tracking, we argue for renewed efforts aimed at cholera prevention to avert more widespread and difficult-to-treat cholera outbreaks.

MATERIALS AND METHODS

Bacterial isolates. A total of 23 bacterial isolates were chosen for whole-genome sequencing based on phenotypic and genetic diversity that was observed during routine molecular surveillance as previously described (26, 17) (see Table S1 in the supplemental material). Clinical isolate C6706, the isogenic Δ*hapR* mutant, and the C6706 derivative carrying *kan* at the *lacZ* site (27) were from our strain collection.

Genome sequence determination. Single-molecule, real-time (SMRT) sequencing was performed on the PacBio *RS* platform using SMRTbell libraries targeting 10-kb inserts using 90-min movies and C2 chemistry (Pacific Biosciences, Menlo Park, CA) using previously established methods and commercially available chemistries (28). Single-end 70- and 100-bp Illumina reads were generated on the GAIIx platform (Illumina, San Diego, CA) using standard procedures.

Genome data acquisition and initial data processing. Illumina runs of publically available genomes were retrieved from the Sequence Read Archive (SRA) and the closed genome of 2010EL-1786 from GenBank (accession numbers NC_016445.1 and NC_016446.1). 2010EL-1786 is an early outbreak isolate from Haiti, which we sequenced, closed, and annotated (7). To improve assembly quality, we trimmed poor quality from the ends of reads and removed reads of bad quality using the script run _assembly_trimClean.pl from CG-Pipeline (CGP) with default options or with a minimum length of 30 bp and no trimming for the 36-bp read sets (29). *De novo* assembly was performed on resulting reads using CGP, which assembles with Velvet (30). Optimal parameters were determined for each assembly using VelvetOptimiser with a *k*-mer range from 27 to

63 bp. Coding gene predictions were prepared with CG-Pipeline, which uses a comprehensive gene prediction approach (29).

Genomes of >4.2 Mb were analyzed for potential contamination by comparing the contigs against the RefSeq database of microbial genomes using BLASTn.

Variant calling and annotation. Illumina reads were mapped against 2010EL-1786 using the SMALT mapper (31), and variants were called with FreeBayes (32). Analysis parameters for calling high-quality SNPs (hqSNPs) were optimized by manually reviewing the pileups versus variant calls for seven random genomes analyzed under different conditions. The following parameters were used: smalt index -k 13 -s 6; smalt map -f samsoft; freebayes --pvar 0 --ploidy 1 --left-align-indels --min-mapping-quality 0 --min-base-quality 20 --min-alternate-fraction 0.75. We removed indels and SNPs with a depth of coverage less than 10 from variant calls. The set of SNPs that passed our filters comprise the final set of hqSNPs used in all subsequent analysis. The set of 45 hqSNPs within the core genome of the Haitian and the three closely related Nepalese genomes were annotated with snpEff (33).

Core genome phylogeny. The Haiti isolates were first examined in a broad phylogenetic context by constructing a tree containing 108 genomes with PhyML using the K80 substitution model, best of NNI and SPR for tree topology searching, and SH-like branch supports (34) (see Fig. S4 in the supplemental material). A phylogeny was constructed for all genomes clustering with the original Haiti genomes (7, 10) plus the three related Nepal genomes (9) using the same approach ($n = 63$).

Bayesian analysis. The analysis of the date for the most recent common ancestor (MRCA) was based on the alignment of 45 hqSNPs from 32 Haiti genomes with known DOCs (see Tables S1 and S2 in the supplemental material). To estimate the date of the outbreak, the sequences were analyzed using BEAST1.72 with an HKY model (35) and 10^8 iterations of the Markov Chain Monte Carlo Simulation. To minimize the number of parameters estimated, we used a strict molecular clock with a starting estimate of 3E-4 hqSNPs/site/day, as estimated by Path-o-Gen (36). We tested three different growth models: constant population size, expansion, and exponential and compared models using Bayes factors based on marginal likelihoods sampled from the posterior. TreeAnnotator, with a burn-in of 1,000 trees, was used to find the best-fitting tree with default parameters.

BLAST atlas. The BLAST atlases were constructed using Illumina-only assemblies relative to a pan-genome, initiated by a concatenated and closed assembly of 2010EL-1786 (accession numbers NC_016445.1 and NC_016446.1). The pangenome for the BLAST atlas was constructed by iterative comparisons of gene predictions from each of the assemblies using BLASTn against the genes in the pangenome set (37). Any genes among the other assemblies which did not have a hit to the pangenome with >80% identity and >100 nucleotides were added to the pangenome set.

Detecting rearrangements with PacBio assemblies. Ten Haiti isolates, including the reference strain 2010EL-1786, were sequenced on the PacBio RS platform using standard C2 chemistry and protocols. For each strain, reference-based alignments as well as de novo assemblies were compared to the closed reference genome of Haiti isolate 2010EL-1786 (7). The reference-based approach to detect structural variants was performed as described previously (28). A novel assembly method was employed that enabled high-quality de novo assembly using solely continuous-long-read (CLR) sequencing data from the PacBio *RS* platform. The assembly pipeline has three main components: preassembly, assembly, and assembly polishing (38).

The preassembly step utilizes the error correction framework from the AHA pipeline (39). However, rather than correcting the long reads with high-quality short reads, as previously described, long reads are used to generate a high-accuracy consensus of other long reads (28). Specifically, the full CLR data set was divided into subsets to include the longest CLRs. The length cutoff for each strain was set to obtain at least 10× corrected read coverage; depending on the sequencing depth and read length pro-

files, these size cutoffs ranged from 4 to 6 kb. This read subset was then corrected using the complete CLR set for each strain.

The resulting corrected (or "preassembled") reads were trimmed to eliminate any low-quality regions in the consensus for each read. The resultant trimmed long reads were then size selected again to obtain at least 10× long-read coverage of the genome (cutoffs ranged from 3 to 6 kb for the preassembled reads). These high-quality reads were passed directly into the Celera Assembler (40).

We performed a final finishing step using Quiver from Pacific Biosciences (https://github.com/PacificBiosciences/GenomicConsensus), which leverages specific quality values and features unique to single molecule sequencing. For each strain, all raw reads were aligned back to the de novo assembled output from the Celera Assembler using BLASR (41). Consensus calling was performed using Quiver to obtain the final finished assemblies.

Sequencing for the superintegron. To validate the PacBio assemblies, we employed Sanger sequencing of the integron region of one isolate. Fosmid libraries were constructed from genomic DNA fragments of 2011EL-2320 using the PCC2FOS Vector (Epicentre, Madison, WI). Libraries were screened using *attC*-targeted primers (reference PMID 17464063) to find integron-containing fragments. Transposons were introduced into the selected fosmids with the EZ-Tn5 <KAN-2> insertion kit (Epicentre) and sequenced using EZ-Tn5-specific primers. Geneious v6.0.3 (Biomatters Ltd., Auckland, New Zealand) was used to assemble sequences to generate the full-length integron sequence. The Sanger consensus sequence was compared to the PacBio assembly.

Confirmation of genome rearrangements. We used PCR to confirm the inversions observed in the CLR assemblies for strains 2011EL-2319, 2011EL-2320, and 2011EL-2323. The sequences around the inversion breakpoints were compared to that of reference strain 2010EL-1786, and nucleotide alignments were viewed in MEGA5 (42). The primer sequences (5′ to 3′) are as follows: 2011EL-2319, GCATTATATC-CCGTCGTTTA and GATCAACTAGCTGGAATAAA; 2011EL-2320, GCATTATATCCCGTCGTTTA and TCTGTCAATGAATACGCAGA; and 2011EL-2323, AGTTTATGATTATGAATAGTGA and GAAACACT AATACAACTAGCC.

Chitin-induced natural transformation assay for HGT. As described previously (13, 14), sterile crab shells in triplicate wells were inoculated with each *V. cholerae* strain in a 12-well plate and provided with 2 μg of genomic DNA (gDNA) marked with a kanamycin resistance (*kan*) gene. Following a 24-h incubation, attached cells were harvested and plated to quantify transformation frequency (TF), defined as *kan* CFU ml^{-1}/total CFU ml^{-1}. Experiments were performed in triplicate. For the experiments whose results are shown in Table 1, each strain was provided with donor gDNA from a C6706 derivative with *kan* at the *lacZ* locus, and the fold TF defect was calculated relative to C6706. In a separate assay (Table 2), twelve pools of donor gDNA were generated from >1,000 Tn5(*kan*) mutants of each isolate, and each pool was used to transform that same isolate and C6706. The fold TF defect was calculated for each isolate relative to C6706 that was also incubated with Tn5(*kan*) gDNA from that isolate. Transposon mutagenesis of C6706 and the Haiti isolates was performed as described elsewhere (43).

Quorum-sensing assay. As described (44), a quorum-sensing reporter plasmid (pBB1) was introduced into each isolate, and then triplicate cultures were grown overnight at 30°C. Luciferase levels and optical density at 600 nm (OD$_{600}$) were determined for each culture to calculate the relative light units (RLUs), expressed as (lux/ml)/(OD$_{600}$ units/ml). A quorum-sensing assay was also performed as previously described (44) (data not shown).

SUPPLEMENTAL MATERIAL

Figure S4, PDF file, 0.1 MB.
Figure S5, PDF file, 0.1 MB.
Figure S6, PDF file, 0.3 MB.
Figure S7, PDF file, 0.8 MB.
Table S1, DOCX file, 0.1 MB.
Table S2, DOCX file, 0.1 MB.
Table S3, DOCX file, 0.1 MB.

REFERENCES

1. **Waldor MK, Mekalanos JJ.** 1996. Lysogenic conversion by a filamentous phage encoding cholera toxin. Science **272**:1910–1914.
2. **Pollitzer R, Swaroop S, Burrows W.** 1959. Cholera. Monogr. S. World Health Organ. **58**:1001–1019.
3. **Mutreja A, Kim DW, Thomson NR, Connor TR, Lee JH, Kariuki S, Croucher NJ, Choi SY, Harris SR, Lebens M, Niyogi SK, Kim EJ, Ramamurthy T, Chun J, Wood JL, Clemens JD, Czerkinsky C, Nair GB, Holmgren J, Parkhill J, Dougan G.** 2011. Evidence for several waves of global transmission in the seventh cholera pandemic. Nature **477**:462–465.
4. **Jenson D, Szabo V, Duke FHI Haiti Humanities Laboratory Student Research Team.** 2011. Cholera in Haiti and other Caribbean regions, 19th century. Emerg. Infect. Dis. **17**:2130–2135.
5. **Barzilay EJ, Schaad N, Magloire R, Mung KS, Boncy J, Dahourou GA, Mintz ED, Steenland MW, Vertefeuille JF, Tappero JW.** 2013. Cholera surveillance during the Haiti epidemic—the first 2 years. N. Engl. J. Med. **368**:599–609.
6. **Chin CS, Sorenson J, Harris JB, Robins WP, Charles RC, Jean-Charles RR, Bullard J, Webster DR, Kasarskis A, Peluso P, Paxinos EE, Yamaichi Y, Calderwood SB, Mekalanos JJ, Schadt EE, Waldor MK.** 2011. The origin of the Haitian cholera outbreak strain. N. Engl. J. Med. **364**:33–42.
7. **Reimer AR, Van Domselaar G, Stroika S, Walker M, Kent H, Tarr C, Talkington D, Rowe L, Olsen-Rasmussen M, Frace M, Sammons S, Dahourou GA, Boncy J, Smith AM, Mabon P, Petkau A, Graham M, Gilmour MW, Gerner-Smidt P, Vibrio cholerae Outbreak Genomics Task Force.** 2011. Comparative genomics of *Vibrio cholerae* from Haiti, Asia, and Africa. Emerg. Infect. Dis. **17**:2113–2121.
8. **Frerichs RR, Keim PS, Barrais R, Piarroux R.** 2012. Nepalese origin of cholera epidemic in Haiti. Clin. Microbiol. Infect. **18**:E158–E163.
9. **Hendriksen RS, Price LB, Schupp JM, Gillece JD, Kaas RS, Engelthaler DM, Bortolaia V, Pearson T, Waters AE, Upadhyay BP, Shrestha SD, Adhikari S, Shakya G, Keim PS, Aarestrup FM.** 2011. Population genetics of *Vibrio cholerae* from Nepal in 2010: evidence on the origin of the Haitian outbreak. mBio **2**:e00157-11. doi:10.1128/mBio.00157-11.
10. **Hasan NA, Choi SY, Eppinger M, Clark PW, Chen A, Alam M, Haley BJ, Taviani E, Hine E, Su Q, Tallon LJ, Prosper JB, Furth K, Hoq MM, Li H, Fraser-Liggett CM, Cravioto A, Huq A, Ravel J, Cebula TA, Colwell RR.** 2012. Genomic diversity of 2010 Haitian cholera outbreak strains. Proc. Natl. Acad. Sci. U. S. A. **109**:E2010–E2017.
11. **Centers for Disease Control and Prevention.** 2012. Notes from the field: identification of *Vibrio cholerae* serogroup O1, serotype Inaba, biotype El Tor strain—Haiti, March 2012. MMWR Morb. Mortal. Wkly. Rep. **61**:309.
12. **Stroeher UH, Karageorgos LE, Morona R, Manning PA.** 1992. Serotype conversion in *Vibrio cholerae* O1. Proc. Natl. Acad. Sci. U. S. A. **89**:2566–2570.
13. **Meibom KL, Blokesch M, Dolganov NA, Wu CY, Schoolnik GK.** 2005. Chitin induces natural competence in *Vibrio cholerae*. Science **310**:1824–1827.
14. **Antonova ES, Hammer BK.** 2011. Quorum-sensing autoinducer molecules produced by members of a multispecies biofilm promote horizontal gene transfer to *Vibrio cholerae*. FEMS Microbiol. Lett. **322**:68–76.
15. **Ivers LC, Walton DA.** 2012. The "first" case of cholera in Haiti: lessons for global health. Am. J. Trop. Med. Hyg. **86**:36–38.
16. **Wozniak RA, Fouts DE, Spagnoletti M, Colombo MM, Ceccarelli D, Garriss G, Déry C, Burrus V, Waldor MK.** 2009. Comparative ICE genomics: insights into the evolution of the SXT/R391 family of ICEs. PLoS Genet. **5**:e1000786. doi:10.1371/journal.pgen.1000786.
17. **Sjölund-Karlsson M, Reimer A, Folster JP, Walker M, Dahourou GA, Batra DG, Martin I, Joyce K, Parsons MB, Boncy J, Whichard JM, Gilmour MW.** 2011. Drug-resistance mechanisms in *Vibrio cholerae* O1 outbreak strain, Haiti, 2010. Emerg. Infect. Dis. **17**:2151–2154.
18. **Chun J, Grim CJ, Hasan NA, Lee JH, Choi SY, Haley BJ, Taviani E, Jeon YS, Kim DW, Lee JH, Brettin TS, Bruce DC, Challacombe JF, Detter JC, Han CS, Munk AC, Chertkov O, Meincke L, Saunders E, Walters RA, Huq A, Nair GB, Colwell RR.** 2009. Comparative genomics reveals mechanism for short-term and long-term clonal transitions in pandemic *Vibrio cholerae*. Proc. Natl. Acad. Sci. U. S. A. **106**:15442–15447.
19. **Ochman H, Lawrence JG, Groisman EA.** 2000. Lateral gene transfer and the nature of bacterial innovation. Nature **405**:299–304.
20. **Grad YH, Godfrey P, Cerquiera GC, Mariani-Kurkdjian P, Gouali M, Bingen E, Shea TP, Haas BJ, Griggs A, Young S, Zeng Q, Lipsitch M, Waldor MK, Weill FX, Wortman JR, Hanage WP.** 2013. Comparative genomics of recent Shiga toxin-producing *Escherichia coli* O104:H4: short-term evolution of an emerging pathogen. mBio **4**:e00452–12. doi:10.1128/mBio.00452-12.
21. **Nguyen BM, Lee JH, Cuong NT, Choi SY, Hien NT, Anh DD, Lee HR, Ansaruzzaman M, Endtz HP, Chun J, Lopez AL, Czerkinsky C, Clemens JD, Kim DW.** 2009. Cholera outbreaks caused by an altered *Vibrio cholerae* O1 El Tor biotype strain producing classical cholera toxin B in Vietnam in 2007 to 2008. J. Clin. Microbiol. **47**:1568–1571.
22. **Grim CJ, Hasan NA, Taviani E, Haley B, Chun J, Brettin TS, Bruce DC, Detter JC, Han CS, Chertkov O, Challacombe J, Huq A, Nair GB, Colwell RR.** 2010. Genome sequence of hybrid *Vibrio cholerae* O1 MJ-1236, B-33, and CIRS101 and comparative genomics with *V. cholerae*. J. Bacteriol. **192**:3524–3533.
23. **Goel AK, Jain M, Kumar P, Bhadauria S, Kmboj DV, Singh L.** 2008. A new variant of *Vibrio cholerae* O1 El Tor causing cholera in India. J. Infect. **57**:280–281.
24. **Kutar BM, Rajpara N, Upadhyay H, Ramamurthy T, Bhardwaj AK.** 2013. Clinical isolates of *Vibrio cholerae* O1 El Tor Ogawa of 2009 from Kolkata, India: preponderance of SXT element and presence of Haitian *ctxB* variant. PLoS One **8**:e56477. doi:10.1371/journal.pone.0056477.
25. **Safa A, Nair GB, Kong RY.** 2010. Evolution of new variants of *Vibrio cholerae* O1. Trends Microbiol. **18**:46–54.
26. **Talkington D, Bopp C, Tarr C, Parsons MB, Dahourou G, Freeman M, Joyce K, Turnsek M, Garrett N, Humphrys M, Gomez G, Stroika S, Boncy J, Ochieng B, Oundo J, Klena J, Smith A, Keddy K, Gerner-Smidt P.** 2011. Characterization of toxigenic *Vibrio cholerae* from Haiti, 2010–2011. Emerg. Infect. Dis. **17**:2122–2129.
27. **Thelin KH, Taylor RK.** 1996. Toxin-coregulated pilus, but not mannose-sensitive hemagglutinin, is required for colonization by *Vibrio cholerae* O1 el Tor biotype and O139 strains. Infect. Immun. **64**:2853–2856.
28. **Rasko DA, Webster DR, Sahl JW, Bashir A, Boisen N, Scheutz F, Paxinos EE, Sebra R, Chin CS, Iliopoulos D, Klammer A, Peluso P, Lee L, Kislyuk AO, Bullard J, Kasarskis A, Wang S, Eid J, Rank D, Redman JC, Steyert SR, Frimodt-Møller J, Struve C, Petersen AM, Krogfelt KA, Nataro JP, Schadt EE, Waldor MK.** 2011. Origins of the *E. coli* strain causing an outbreak of hemolytic-uremic syndrome in Germany. N. Engl. J. Med. **365**:709–717.
29. **Kislyuk AO, Katz LS, Agrawal S, Hagen MS, Conley AB, Jayaraman P, Nelakuditi V, Humphrey JC, Sammons SA, Govil D, Mair RD, Tatti KM, Tondella ML, Harcourt BH, Mayer LW, Jordan IK.** 2010. A computational genomics pipeline for prokaryotic sequencing projects. Bioinformatics **26**:1819–1826.
30. **Zerbino DR, Birney E.** 2008. Velvet: algorithms for de novo short read assembly using de Bruijn graphs. Genome Res. **18**:821–829.
31. **Ponstingl H, Ning Z.** 2010. SMALT—a new mapper for DNA sequencing reads. F1000 Posters **1**:313.

32. **Garrison E, Marth G.** 2012. Haplotype-based variant detection from short-read sequencing. arXiv 1207.3907.

33. **Cingolani P, Platts A, Wang LL, Coon M, Nguyen T, Wang L, Land SJ, Lu X, Ruden DM.** 2012. A program for annotating and predicting the effects of single nucleotide polymorphisms, SnpEff: SNPs in the genome of *Drosophila melanogaster* strain w1118; iso-2; iso-3. Fly **6:**80–92.

34. **Guindon S, Dufayard JF, Lefort V, Anisimova M, Hordijk W, Gascuel O.** 2010. New algorithms and methods to estimate maximum-likelihood phylogenies: assessing the performance of PhyML. Syst. Biol. **59:**-307–321.

35. **Drummond AJ, Suchard MA, Xie D, Rambaut A.** 2012. Bayesian phylogenetics with BEAUti and the BEAST. Mol. Biol. Evol. **29:**-1969–1973.

36. **Rambaut A.** 2009. Path-O-Gen. http://tree.bio.ed.ac.uk/software/pathogen.

37. **Camacho C, Coulouris G, Avagyan V, Ma N, Papadopoulos J, Bealer K, Madden TL.** 2009. BLAST +: architecture and applications. BMC Bioinformatics **10:**421.

38. **Chin CS, Alexander DH, Marks P, Klammer AA, Drake J, Heiner C, Clum A, Copeland A, Huddleston J, Eichler EE, Turner SW, Korlach J.** 2013. Nonhybrid, finished microbial genome assemblies from long-read SMRT sequencing data. Nat. Methods **10:**563–569.

39. **Bashir A, Klammer AA, Robins WP, Chin CS, Webster D, Paxinos E, Hsu D, Ashby M, Wang S, Peluso P, Sebra R, Sorenson J, Bullard J, Yen J, Valdovino M, Mollova E, Luong K, Lin S, LaMay B, Joshi A, Rowe L, Frace M, Tarr CL, Turnsek M, Davis BM, Kasarskis A, Mekalanos JJ, Waldor MK, Schadt EE.** 2012. A hybrid approach for the automated finishing of bacterial genomes. Nat. Biotechnol. **30:**701–707.

40. **Koren S, Schatz MC, Walenz BP, Martin J, Howard JT, Ganapathy G, Wang Z, Rasko DA, McCombie WR, Jarvis ED, Adam MP.** 2012. Hybrid error correction and de novo assembly of single-molecule sequencing reads. Nat. Biotechnol. **30:**693–700.

41. **Chaisson MJ, Tesler G.** 2012. Mapping single molecule sequencing reads using basic local alignment with successive refinement (BLASR): application and theory. BMC Bioinformatics **13:**238.

42. **Tamura K, Peterson D, Peterson N, Stecher G, Nei M, Kumar S.** 2011. MEGA5: molecular evolutionary genetics analysis using maximum likelihood, evolutionary distance, and maximum parsimony methods. Mol. Biol. Evol. **28:**2731–2739.

43. **Antonova ES, Bernardy EE, Hammer BK.** 2012. Natural competence in *Vibrio cholerae* is controlled by a nucleoside scavenging response that requires CytR-dependent anti-activation. Mol. Microbiol. **86:**1215–1231.

44. **Miller MB, Skorupski K, Lenz DH, Taylor RK, Bassler BL.** 2002. Parallel quorum sensing systems converge to regulate virulence in *Vibrio cholerae*. Cell **110:**303–314.